

Development of Compact Permanent Magnet Electron Focusing Devices

A Project Report
in the programme of

Research Program for International Talents (PSEI) - 2023

submitted towards

**Dept. of Science & Technology (DST), Govt. of India
Scholarship for Higher Education (SHE)**

by

SUMIT KUMAR NAYAK

SHE Scholar IVR Number : **201900031348**

Indian Institute of Technology Delhi (IIT-D)



**ECOLE POLYTECHNIQUE
PALAISEAU - 91120 , FRANCE**

[May - August 2023]

ACKNOWLEDGEMENT

I want to extend a sincere and heartfelt obligation towards all the personages without whom the completion of the project was not possible. I express my profound gratitude and deep regard to Dr. Arnd Specka, Ecole Polytechnique for his continuous guidance, valuable feedback, and constant encouragement throughout the project duration. His intuitiveness and insight has been invaluable to the progression of this project, allowing it to mature into the project it is today. I also acknowledge to all other GALOP & LLR-Mechanique team-members at Polytechnique for their utmost support and considerable assistance during the project.

I am immensely grateful to Polytechnique Authorities for their constant assistance and encouragement. I am also grateful to Polytechnique International Relation Program Committee and Ms. Nathalie Legeay & Maria Dubiel, the coordinator of PSEI Program for allowing me to do this project and providing all the required facilities. Last but not the least, I am also indebted to my Parents and the Almighty Lord Jagannath, whose blessings helped me to carry out such a wonderful project smoothly.



Sumit Kumar Nayak

Route De Saclay -91120

Contents

1	Introduction	1
1.1	Overview of LPA System	1
1.2	Aim of this Project	1
2	Basic Interpretation	3
2.1	Factors that we are looking into	3
2.1.1	Gradient	3
2.1.2	Skew Angle	3
2.1.3	Magnetic Centre	4
2.1.4	Chi-Squared Value	4
2.2	Scrutinising the Primary Data	4
2.2.1	Plotting Field vs Position : B_x vs Y, B_y vs X, B_z vs Z	4
2.2.2	Intensity Plot at Z-plane	6
3	Experimental Setup & Steps	8
3.1	Knowing the Table-top Arrangement	8
3.1.1	Hardware Instruments	8
3.1.2	Software Tools	9
3.2	Working Instructions	9
3.3	Extracting Data for Use	9
4	Probe Analysis	11
4.1	Separate Linear Fit	11
4.1.1	Defining Fitting Function	11
4.1.2	Parameters Calculation	11
4.1.3	Results	13
4.2	Common (Simultaneous) Fit	14
4.2.1	6 - Parameter Common Fit	15
4.2.2	4 - Parameter Common Fit	15
4.2.3	Parameter Calculation	15
4.2.4	Results	17
4.3	Error Comparison between Common and Separate fit	18
4.4	Fitting Including Z-component	19
4.4.1	6 - Parameter Common Fit (All 3 component)	20
4.4.2	4 - Parameter Common Fit (All 3 component)	20
4.4.3	Parameter Calculation	21
5	Advanced Probe Analysis	23

5.1	Enge Parametrisation	23
5.1.1	Power Law fit to Enge's Function	24
5.1.2	Linear Power Law Fit	25
5.1.3	Results	26
5.2	Developing Theory for Non-Linear Fit	26
5.2.1	Method of 2D Taylor Expansion	26
5.2.2	Concept of Multipole Expansion	27
5.2.3	Method of Multipole Expansion	28
6	Conclusion	29

List of Figures

1.1	Schematics of LPA System	2
2.1	Field vs Coordinates for 18mm bore Magnet	5
2.2	Field vs Coordinates for 30mm bore Magnet	5
2.3	Field Intensity : 18mm Magnet	6
2.4	Field Intensity : 30mm Magnet	7
4.1	Separate Fit Analysis : 18mm Magnet (QPMLLR-02)	13
4.2	Separate Fit Analysis : 30mm Magnet (QPMLLR-03)	14
4.3	Common fit Analysis :18 mm Magnet	16
4.4	Common fit Analysis :30 mm Magnet	17
4.5	Error Calculation : 18mm Magnet	18
4.6	Error Calculation : 30mm Magnet	19
4.7	Three component fitting : 18mm Magnet	21
4.8	Three component fitting : 30mm Magnet	22
5.1	Enge Gradient : 18mm Magnet	25
5.2	Enge Gradient : 30mm Magnet	26

List of Tables

5.1	Enge's Parametrisation for QPM-LLR-02 (18mm)	24
5.2	Enge's Parametrisation for QPM-LLR-03 (30mm)	24
5.3	Power Law Parametrisation for QPM-LLR-02 (18mm)	24
5.4	Power Law Parametrisation for QPM-LLR-03 (30mm)	25

Chapter 1

Introduction

1.1 Overview of LPA System

Apart from conventional Linear RF accelerators, the Laser-driven Plasma Accelerator (**LPA**) is a type of particle accelerator system that utilizes intense laser beams to generate plasma waves. These plasma waves are indeed particle bunches (ions or electrons), which are then accelerated to very high energies over very short distances.

Basically A high-intensity laser pulse is focused onto a target material, typically a suitable gas, creating a plasma. The intense laser field ionizes the gas medium, ionising electrons from atoms and creating a plasma of charged particles. The laser is responsible for creating a highly nonlinear electrostatic field known as "*Wakefield*". When charged particles interact with the wakefield, they gain energy and accelerate to very high velocities. This entire phenomena of accelerating to velocities close to the speed of light within very short distances, often measured in few meters. This is in contrast to conventional particle accelerators, which can be kilometers in length.

One important aspect for the system to perform optimally is to ensure that the electron beam passes through the geometric axis of the beam line, however this may not be achieved in a real system. Therefore electron focusing devices are employed to give requisite corrections to the beam trajectory. The details about this focusing device is discussed vividly in the following sections.

1.2 Aim of this Project

From above system description, it is seen that highly energetic electron bunch generated from plasma are strongly divergent. There may be a few reasons behind this divergent nature of the accelerating particle bunch such as Spatial charge repulsion, offset generation point etc. Once a bunch generated with some angle with respect to the beam axis will eventually be lost before reaching the target, if not corrected.

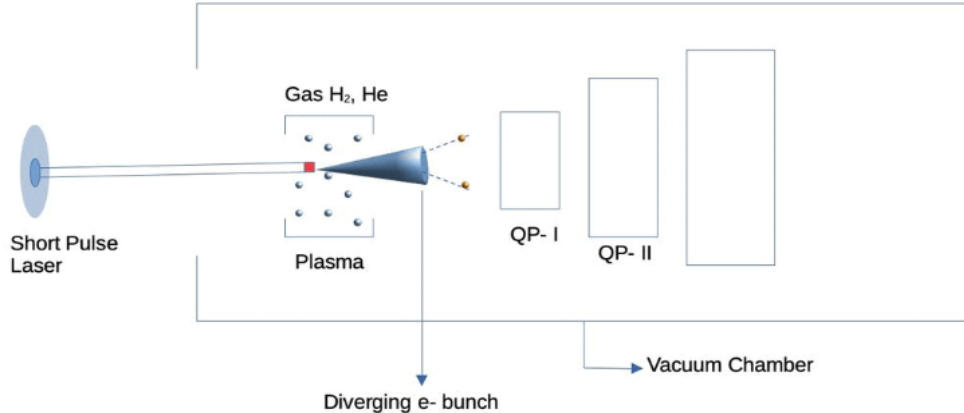


Figure 1.1: Schematics of LPA System

Thus, our aim is to create and test such a Electron Focusing device which will correct the divergence of electron beam. This is achieved through using **set of Quadrupole Magnets (QPMs)** on the beam axis as shown in the fig 1.1. The basic function of a quadrupole magnet is to focus in one axis and de-focus in the other, when the bunch travels through its magnetic axis. With help of Ion Beam Optics, we can position these magnet in such a position that, it will focus the beam in each standard direction turn by turn.

Thus we can ensure that the beam entering the bore volume of the QPMs are emerged as focused beam after their exit.

Chapter 2

Basic Interpretation

From very basic formulation of the magnetic fields of quadrupoles, it is formulated ideally as [5]:

$$\begin{aligned} B_x &= G \times Y \\ B_y &= G \times X \end{aligned} \quad (2.1)$$

Where, G is the **Gradient** of the field B_x & B_y are the components of the magnetic field in X and Y direction, respectively. A typical quadrupole that we are using will be the magnitude of 1-2 Tesla with a gradient value that varies around 0.1 - 0.2 T/mm, where Gradient defined as

$$G = \frac{B_{tip} \text{ (Tesla)}}{R_{bore} \text{ (Metre)}} \quad (2.2)$$

2.1 Factors that we are looking into

In our analysis process, we will look for several parameters that characterize the requisite functioning of the Quadrupole magnet. Those are described as follows :

2.1.1 Gradient

As formulated in the Eqn.2.1, Gradient is like slope of the straight line function. For an ideal magnet it should be some fixed constant value (which is Tip saturated field in our case), will be shown later in the graphs. But, in the rapid changing fields, one may expect varying gradient values.

2.1.2 Skew Angle

No matter, how precise you align the magnet and probe on a fixed axis, there will be limitation to mechanical precision. So, this small slant in the magnet or in the probe creates a tilted direction measurement. This angular deviation between the coordinate system of magnet and probe results the magnitude of the skew angle.

2.1.3 Magnetic Centre

For a symmetric scan, we always begin with our reference from the central axis in the bore volume. Thus, we define probe origin before the scan rolls out (*Detailed description in the Alignment Instruction*). However, our so called probe origin may/may not be coincident with the actual magnetic centre of the magnet.

In that case, we will observe some non-zero values, at our defined probe origin coordinates, while the ideal quadrupole has zero values at origin. This offset measurement tells about the precision of alignment in the accordance of mechanical perfection.

2.1.4 Chi-Squared Value

This is a statistical method used to compare observed results with expected results. The purpose of this calculation is to determine if a difference between observed data and expected data is due to chance, or if it is due to a relationship between the variables you are studying.

2.2 Scrutinising the Primary Data

Before going in to the detailed calculation of these parameters, one should have a primary check on the measured data sets. These basic checking methods, will yield a brief idea about existence of outliers (if any) and cross verify the behaviour of the field pattern according to the theoretical interpretation.

2.2.1 Plotting Field vs Position : B_x vs Y, B_y vs X, B_z vs Z

From the ideal expression of a quadrupole i.e. Eqn 2.1, plot for B_x & B_y should follow up some straight line graph. If one has, multiple number of measurements at fix X & Y values, then mean value of the field at particular X & Y values follows the straight line. This straight line will pass through the origin if our magnet is Ideal. Else, the deviation can be accounted for outliers or some alignment precision.

In comparison to the B_x, B_y the magnitude of B_z is small. These Two peak occurs in the fringe field i.e. regions just around the exit planes of the magnet, where field changes rapidly. This graph contains the information regarding numerical derivative of the field gradient as field in Z-component given as :

$$B_z = G' \times X.Y \quad (2.3)$$

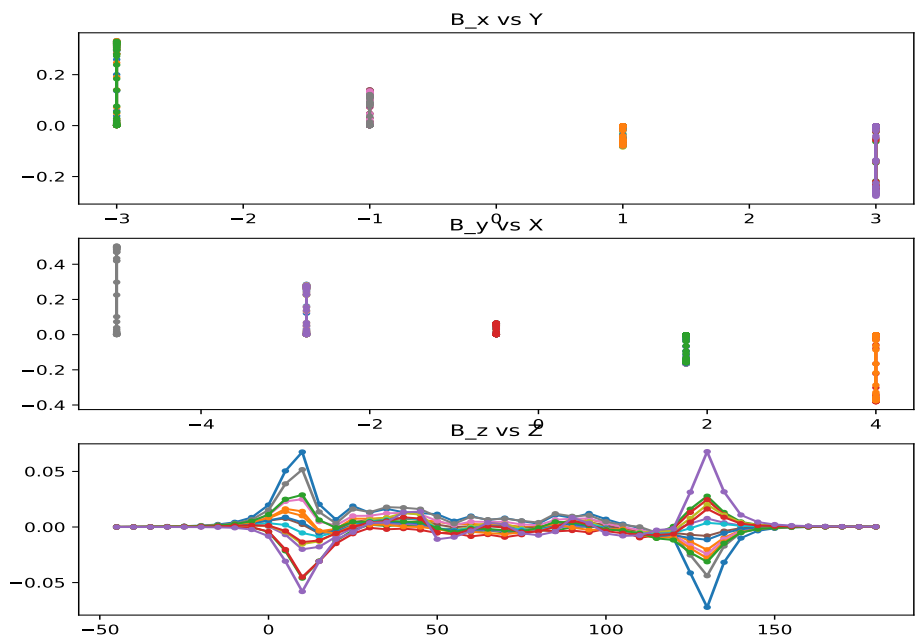


Figure 2.1: Field vs Coordinates for 18mm bore Magnet

for 30 mm magnet :

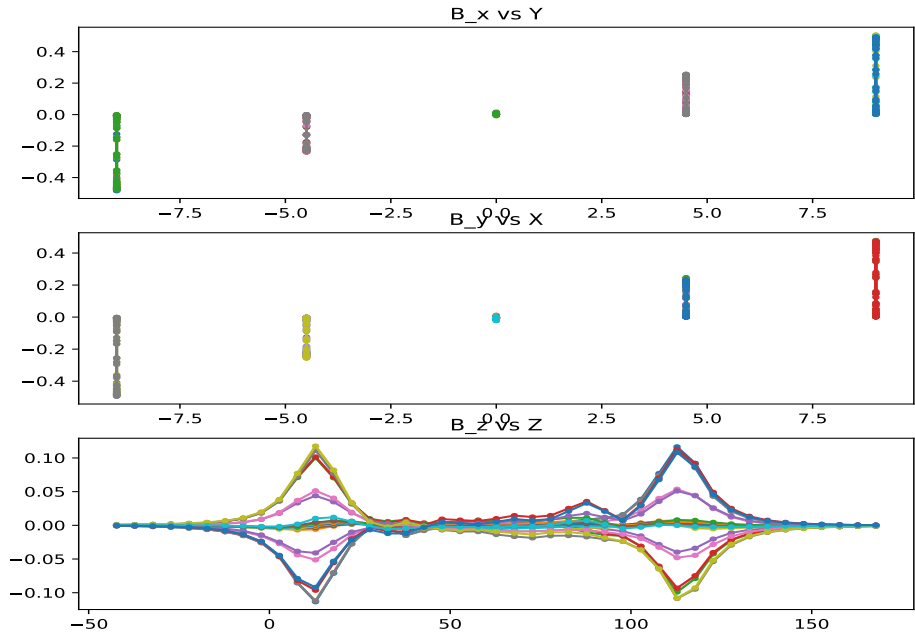


Figure 2.2: Field vs Coordinates for 30mm bore Magnet

2.2.2 Intensity Plot at Z-plane

Squaring and adding up the expressions from eqn-2.1, it will be simplified to :

$$\begin{aligned} B_x^2 + B_y^2 &= G^2(X^2 + Y^2) \\ \frac{\sqrt{B_x^2 + B_y^2}}{G} &= \frac{B_{net}}{G} = \frac{(X^2 + Y^2)}{G} \end{aligned} \quad (2.4)$$

not correct, should be square

Considering the ratio ($\frac{B_{net}}{G}$) to be a fixed number, it should look like a equation of **Circle**. Ideally, when we plot this square root sum of square of the fields, it should look like a circle centered at the bore centre. Any abnormality in the structure implies field has strong implication from sextupole and octupole components [3]. Higher the deviation from the circular configuration, larger the higher magnetic moments.

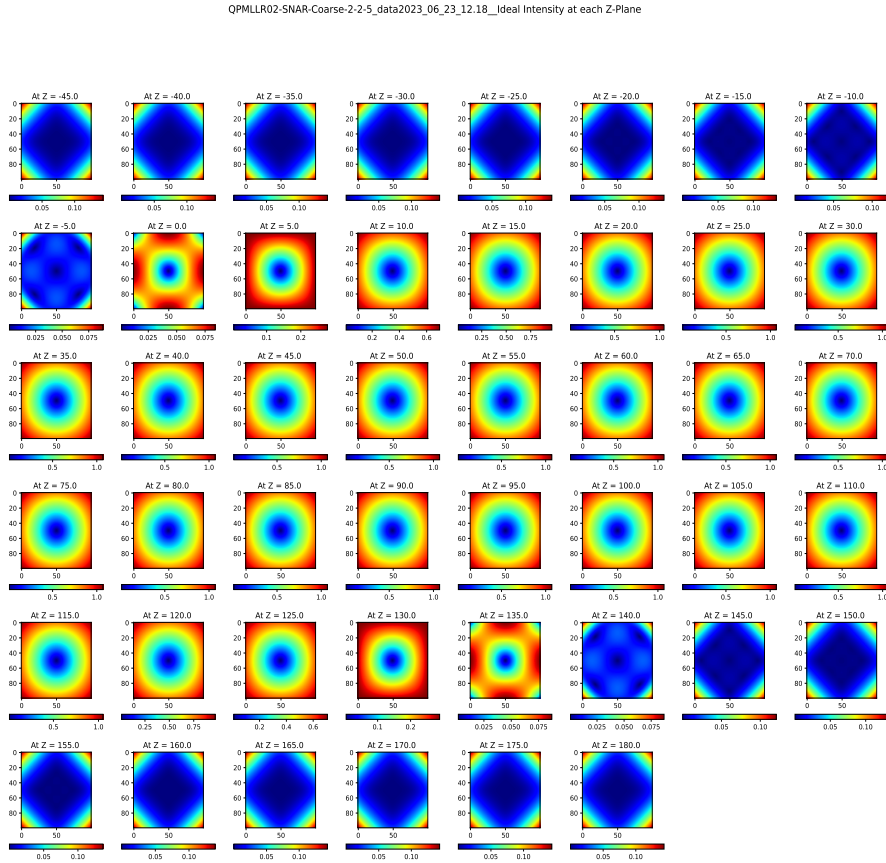


Figure 2.3: Field Intensity : 18mm Magnet

Doing same for the 30 mm magnet (QPM-LLR-03)

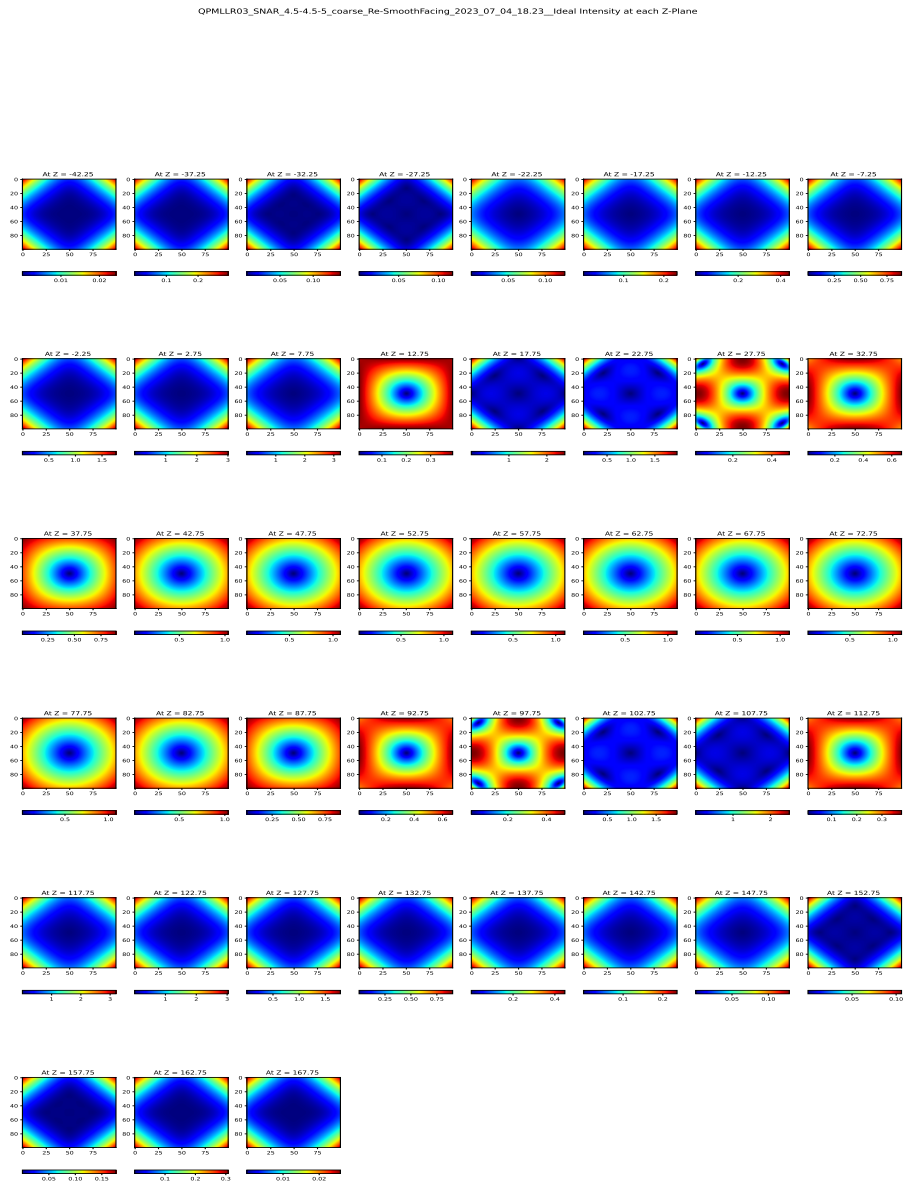


Figure 2.4: Field Intensity : 30mm Magnet

Chapter 3

Experimental Setup & Steps

3.1 Knowing the Table-top Arrangement

As we will be working on one magnet at a time, there is no need of very large setup area. One can follow up the figure 5.2 below, We have very few number of major apparatus in our setup. They are :

3.1.1 Hardware Instruments

1. **Laser** :- This laser beam is aligned as parallel with the top of experimental table. Then, path of Laser is taken as reference for the central axis of movement of the probe tip. Also, we can adjust position of the magnet according to the level of this laser.
2. **Iris** :- Through the iris, one can adjust the spot size of the laser beam. Basically, one can control the brightness of the laser according to the requisite level.
3. **Reflecting Mirror** :- As laser is kept on the different direction from the probe and magnet, set of these mirrors are used for directing laser beam to fall appropriately on the probe tip
4. **Semi Transparent Beam Splitter** :- It is considered as common pathways for laser and camera view. Due to semi-transparency laser passes smoothly from reflecting mirror to probe. On the other hand, reflecting portion helps to have a wider view range for the camera.
5. **High Resolution Camera** :- Camera is used to adjust the alignment via visual perception at maximum. Mainly, bore origin is determined through the pixel counting.
6. **Magnet** :- In our case, we will be using different types of **Quadrupole Magnets** prototypes, which are discussed in the earlier sections.
7. **Magnet Table/Rotatory Holder** :- It is useful for placing the magnet in the requisite level with different angular orientation.

8. **Three Stage Motor with Holder** :- 3-stage is used for dynamical Cartesian movement of the probe. Each X,Y & Z axis is attached along independent motor stage of micro-steps precision.
9. **Hall Probe** :- A device, combined with associated electronics, which is used to measure the magnetic field based on the phenomena of Hall effect.
 - **3D Hall Probe** :- Measuring Field in all 3- direction simultaneously
 - **1D - Thick & Long Probe**:- One direction measurement for medium size magnets
 - **1D - Thin & Short Probe** :- Measurement for smaller size magnets

3.1.2 Software Tools

Basically, we will be using **TWO** software interfaces. One for handling the camera view and other for controlling the movement of the motor stage. The software's developed by the IT specialists from the LLR Lab. They are :-

- **Pylon App Viewer** :- To plug in camera and capture the continuous photographs along with grid line features
- **Galop GUI** :- Interface for coordinate inputs and speed control of the motorstage

3.2 Working Instructions

On a brief note, laser passes through iris, deviated by reflecting mirrors crosses the bore volume and reaches to the probe tip. We have used Camera view to adjust the same. Once the alignment is done, probe coordinated are defined through the GUI interface and Scan started.

3.3 Extracting Data for Use

Once the probe scan is completed, data is stored in the several columns simultaneously.

Now, to study different aspects of the B_x, B_y & B_z along with X,Y & Z positions, data is extracted as several numbers of arrays and lists. These were done in **TWO** different methods.

- **Appending Nested Lists** :- Less Pythonic / More like C++ algorithm
In this method, we have created required number of blank lists. Then in nested for loop, data is read row-wise and appended to the respective blank variable lists as per defined indices.
- **In built Command `(np.genfromtxt)`** :- More Pythonic Way
Using single command line, each column data is extracted as arrays in this case. Obtaining data directly as arrays, makes life more simpler and code shorter.

Apart from the defining different variables, these two methods are developed in such a standard way that it can be directly used as extracting data from different columns. Keeping the variable fields fixed, these two methods can be treated as BLACK-BOX which transform ASCII data to the list of arrays.

Chapter 4

Probe Analysis

4.1 Separate Linear Fit

4.1.1 Defining Fitting Function

From earlier discussion, we know that each field component is linearly proportional to the complement position (i.e. $B_x \propto Y$ and $B_y \propto X$) ideally. In a fixed Z-plane; to check whether there is an contribution from the other position component, we have designed the equations as follows :

$$B_x = B_{00}^x + (B_{10}^x)X + (B_{01}^x)Y \quad (4.1)$$

$$B_y = B_{00}^y + (B_{10}^y)X + (B_{01}^y)Y \quad (4.2)$$

Where, each coefficients stand as

B_{00}^x, B_{00}^y = Intercept value for linear fitting

B_{10}^x, B_{10}^y = Field gradient in X-coordinates

B_{01}^x, B_{01}^y = Field gradient in Y-coordinates

In our nomenclature, this fitting is called **Separate Linear Fit** as the eqn 4.1 & eqn 4.2 fits the data separately for each component of X and Y at a fixed Z-plane. Once the data were extracted, positional arrays of X & Y fed in to the equations through Python Scipy Curve_fit command. Then corresponding measured field values are minimised through in-built least square fitting method and unknown coefficients values are determined. In the similar way, it is done for each Z-slices & values of six parameters are saved in a list.

4.1.2 Parameters Calculation

Chi-square of Fit

Once the unknown coefficients values are determined form the fit, expected B_x, B_y values are calculated using same fitting function[1][2]. Then, square error between expected and measured values are summed up for a single Z-plane data points along with the consideration of constant precision error of 10^{-4} order. For all fits, we have

considered the following :

$$\chi^2 = \frac{(B_{measured} - B_{fitted})^2}{Error^2} \quad (4.3)$$

This, chi-square values are more important as they will be a standard for comparison of better fits.

Gradient & Skew Angle

Ideally let's assume, both the field component has same Field gradient and skew angle. So we can rewrite eqn 2.1 as

$$\begin{aligned} B_x &= B_{00}^x + GY' \\ B_y &= B_{00}^y + GX' \end{aligned} \quad (4.4)$$

Now, inserting coordinate rotation transformation with angle α as

$$\begin{bmatrix} X' \\ Y' \end{bmatrix} = \begin{bmatrix} \cos(\alpha) & -\sin(\alpha) \\ \sin(\alpha) & \cos(\alpha) \end{bmatrix} \times \begin{bmatrix} X \\ Y \end{bmatrix} \quad (4.5)$$

The above equation 4.4 is transformed into

$$\begin{aligned} B_x &= B_{00}^x + (G \cdot \sin(\alpha))X + (G \cdot \cos(\alpha))Y \\ B_y &= B_{00}^y + (G \cdot \cos(\alpha))X - (G \cdot \sin(\alpha))Y \end{aligned} \quad (4.6)$$

The above equation will be used as parametric fit, discussed in further section. For our convenience, in Separate fit method, we have used gradient & skew angle along with the respective component subscript. Thus, above eqn 4.6 can be re-written as

$$\begin{aligned} B_x &= B_{00}^x + (G_x \cdot \sin(\alpha_x))X + (G_x \cdot \cos(\alpha_x))Y \\ B_y &= B_{00}^y + (G_y \cdot \cos(\alpha_y))X - (G_y \cdot \sin(\alpha_y))Y \end{aligned} \quad (4.7)$$

Comparing eqn 4.7 and 4.1 & 4.2 ; we conclude the following equations.

$$\begin{aligned} B_{10}^x &= G_x \sin \alpha_x \\ B_{01}^x &= G_x \cos \alpha_x \\ B_{10}^y &= G_y \cos \alpha_y \\ B_{01}^y &= -G_y \sin \alpha_y \end{aligned} \quad (4.8)$$

Now, these 4 set of equation can be solved in two ways. They are :

- **Analytical Method :** Squaring-adding & dividing each pair of equation 4.8; we can obtain the values as

$$\begin{aligned} G_x &= \sqrt{B_{10}^{x^2} + B_{01}^{x^2}}; \quad \alpha_x = \arctan \left(\frac{B_{10}^x}{B_{01}^x} \right) \\ G_y &= \sqrt{B_{10}^{y^2} + B_{01}^{y^2}}; \quad \alpha_y = \arctan \left(\frac{B_{10}^y}{B_{01}^y} \right) \end{aligned} \quad (4.9)$$

- **fsolve Command :** Out of four equations above we can solve each pair of simultaneous equations for two variables that is (G_x, α_x) and (G_y, α_y) . This can be achieved by fsolve in-built command of Python.

Magnetic Centre

In an ideal condition, field at magnetic centre is zero (as the opposite direction value cancels out each other). From fitting we can see that B_{10}^x, B_{01}^y coefficients are negligible. Ignoring these two coefficients, setting up LHS = 0 in eqn 4.1 & 4.2 gave us;

$$Y_c = - \left(\frac{B_{00}^x}{B_{01}^x} \right) \quad X_c = \left(\frac{B_{00}^y}{B_{10}^y} \right) \quad (4.10)$$

4.1.3 Results

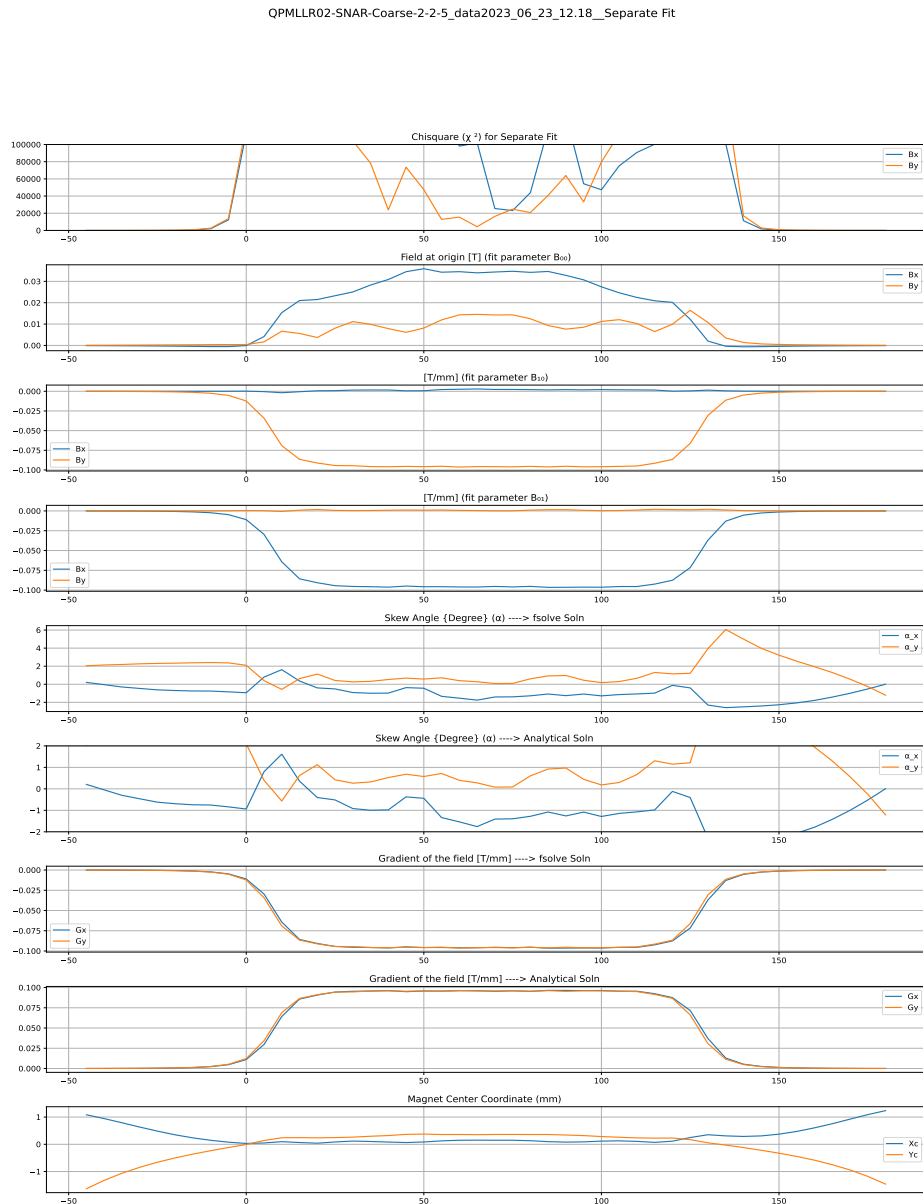


Figure 4.1: Separate Fit Analysis : 18mm Magnet (QPMLLR-02)

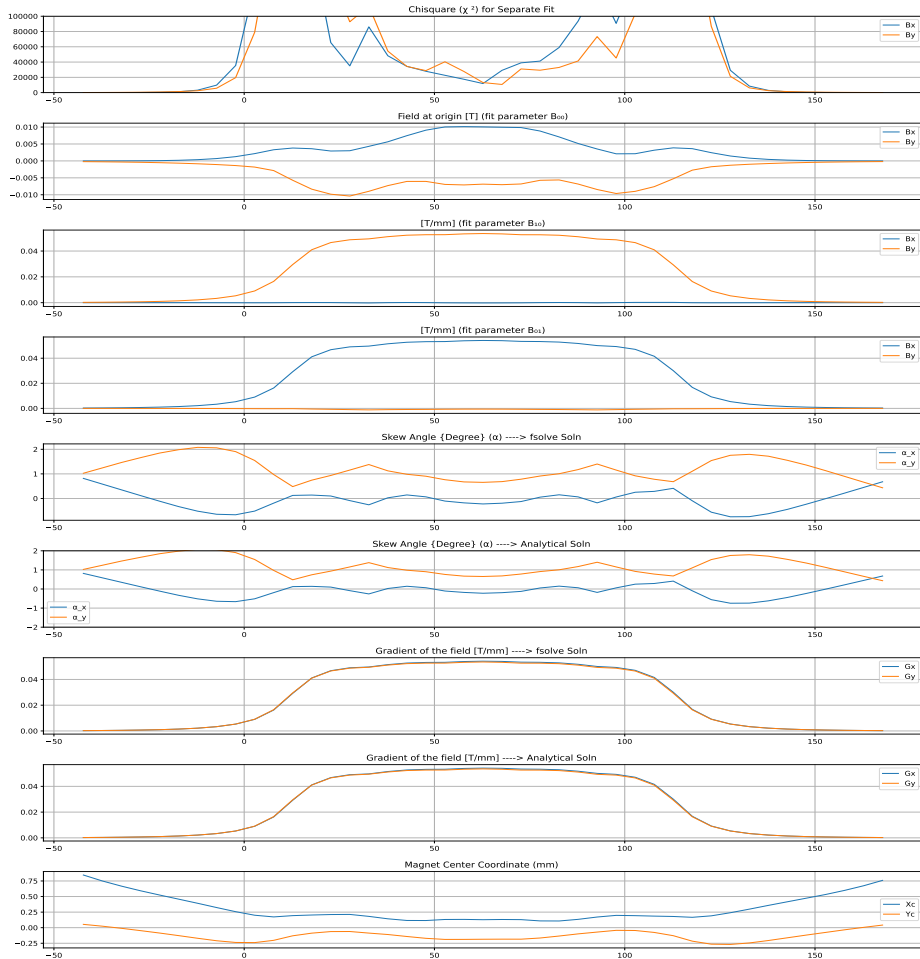


Figure 4.2: Separate Fit Analysis : 30mm Magnet (QPMLLR-03)

In the earlier section, we have tried to fit each component separately & independently. But, in the simultaneous fit we will concatenate each components in to single array & then directly go for the minimisation of all the parameters simultaneously. This was done to check whether there is any change in the estimated values of same parameters while fitting in a different manner.

4.2 Common (Simultaneous) Fit

In the previous section we have fitted each component of magnetic field separately. That means unknown coefficients in the eqn 4.1 and 4.2 are optimized separately. Now we are more interested to optimize all of the unknowns in a single stretch. Let follows How ??

For this purpose, we tried to optimize the coefficients by **Least Square Fitting**

method. In this way, we have defined the fitting function as earlier we have used and then given Python `least_squares` command from `scipy.optimize` library.

4.2.1 6 - Parameter Common Fit

Here, we will be using both the eqn 4.1 and 4.2, but in a different manner. We will concatenate B_x & B_y matrix to a single array and try to optimize six unknowns in the equations altogether. Concatenation for a single Z-plane is done as follows (plane having n number of measured points) :

$$\begin{bmatrix} B_{x1} \\ B_{x2} \\ \dots \\ B_{xn} \\ B_{y1} \\ B_{y2} \\ \dots \\ B_{yn} \end{bmatrix} = \begin{bmatrix} B_{00}^x + (B_{10}^x)X_1 + (B_{01}^x)Y_1 \\ B_{00}^x + (B_{10}^x)X_2 + (B_{01}^x)Y_2 \\ \dots \\ \dots \\ B_{00}^y + (B_{10}^y)X_1 + (B_{01}^y)Y_1 \\ B_{00}^y + (B_{10}^y)X_2 + (B_{01}^y)Y_2 \\ \dots \\ \dots \\ B_{00}^y + (B_{10}^y)X_n + (B_{01}^y)Y_n \end{bmatrix} \quad (4.11)$$

Doing the similar process of fitting for each Z-plane, determined coefficients value appended in individual empty list for further parameter calculations.

4.2.2 4 - Parameter Common Fit

This method of fitting the data set is moreover analogous to the discussion in section 4.2.1. The only difference will be the number of unknown coefficients in the case and parametric equations used. With eqn 4.6, fitting is done in the following form :

$$\begin{bmatrix} B_{x1} \\ B_{x2} \\ \dots \\ B_{xn} \\ B_{y1} \\ B_{y2} \\ \dots \\ B_{yn} \end{bmatrix} = \begin{bmatrix} B_{00}^x + (G \cdot \sin(\alpha))X_1 + (G \cdot \cos(\alpha))Y_1 \\ B_{00}^x + (G \cdot \sin(\alpha))X_2 + (G \cdot \cos(\alpha))Y_2 \\ \dots \\ \dots \\ B_{00}^y + (G \cdot \cos(\alpha))X_1 - (G \cdot \sin(\alpha))Y_1 \\ B_{00}^y + (G \cdot \cos(\alpha))X_2 - (G \cdot \sin(\alpha))Y_2 \\ \dots \\ \dots \\ B_{00}^y + (G \cdot \cos(\alpha))X_n - (G \cdot \sin(\alpha))Y_n \end{bmatrix} \quad (4.12)$$

Again, calculated unknown coefficients are appended in empty list for each Z-plane values.

4.2.3 Parameter Calculation

Few of parameters are calculated directly from the fitting function and few are derived from the further formulating fitting values. Doing fitting for each Z-plane, values for entire scanning volume is obtained.

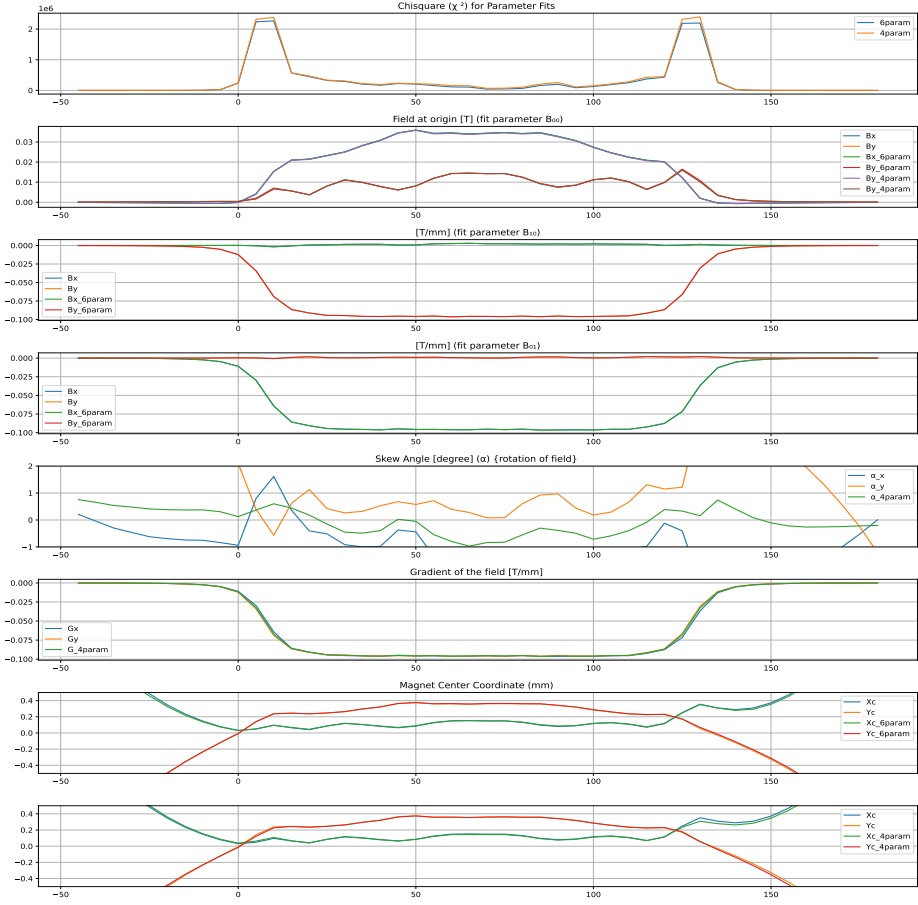


Figure 4.3: Common fit Analysis :18 mm Magnet

Field at Origin (B_{00}), Component wise Gradient (B_{10}, B_{01})

These three parameters are directly computed from the 6-parameter fit.

Overall Gradient (G) & Skew Angle (α)

These two parameters obtained directly from 4-parameter fit and then compared to the value obtained from Separate fit.

Magnetic Center (X_c, Y_c)

From the definition given in the section 2.1.3, Magnetic Centre are those points at which magnetic field is zero. Let consider any Z-plane, in 6-parameter common fit. Once we obtain coefficient values, putting LHS = 0 (Zero) in eqn 4.1 and 4.2; it becomes simultaneous equation in two variables of X, Y. Solution of these two

equations yield coordinates of magnetic centre for that particular plane.

$$0 = B_{00}^x + (B_{10}^x)X + (B_{01}^x)Y$$

$$0 = B_{00}^y + (B_{10}^y)X + (B_{01}^y)Y$$

This can be re-iterated for all Z-planes in scanning volume. By the same analogy, we have also put LHS to Zero in eqn 4.6 and obtained centre's coordinate from 4-parameter common fit.

4.2.4 Results

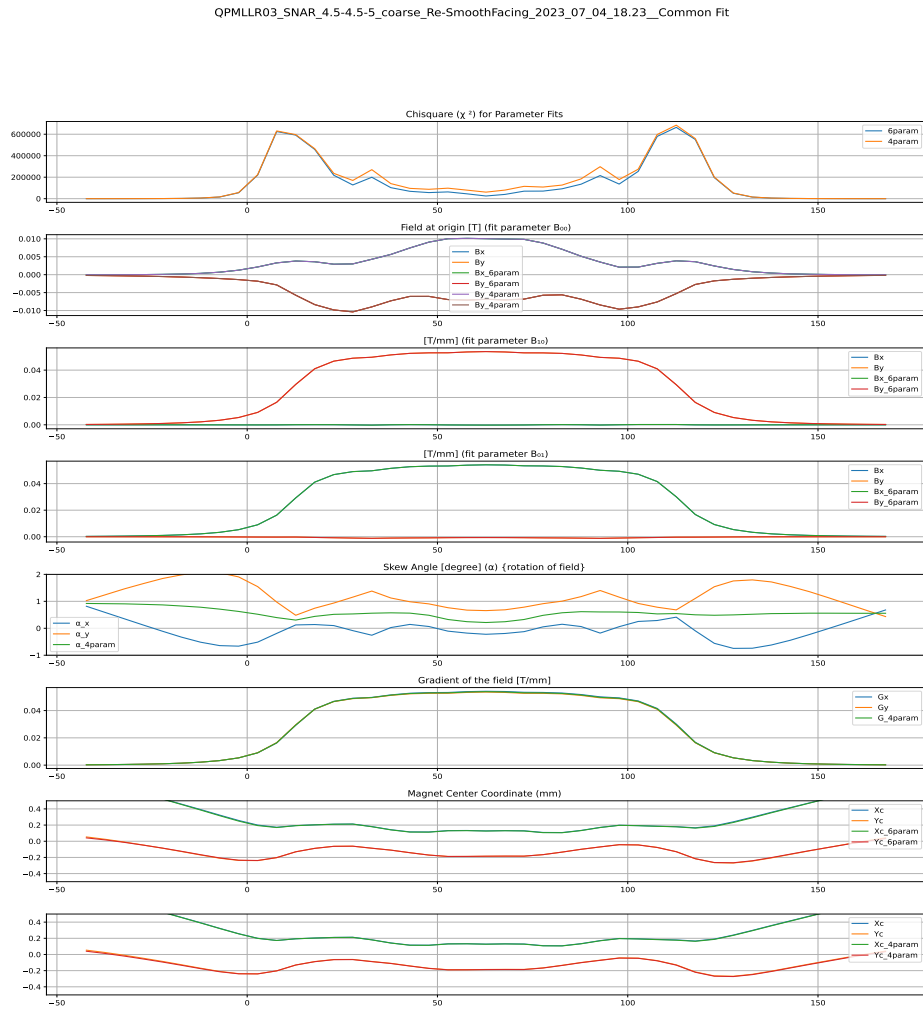


Figure 4.4: Common fit Analysis :30 mm Magnet

4.3 Error Comparison between Common and Separate fit

In the earlier sections of 4.2.2, 4.2.1 and 4.1.1, we have discussed different type of fitting methods. From each type of fitting we have calculated all those same set of parameters for each Z-planes in the scanning volume. Thus, we are interested for the relative error in the calculated parameters with respect to the very first method of the Separate fit. Let \mathbf{A} be any calculated parameter; then **percent relative error**(for a fixed Z-plane) defined as :

$$\% \text{ Relative Error} = \left| \frac{A_{\text{fitting}} - A_{\text{separate fit}}}{A_{\text{separate fit}}} \right| \times 100 \quad (4.13)$$

Where A_{fitting} can be any corresponding parameter from 4 - parameter or 6 - parameter fitting.

NOTE : As Skew angle are nearly zero, so a slight deviation in the value (in fractions of degree) leads to a larger value of relative error. So, we have only calculated **direct difference** from the values of separate fit.



Figure 4.5: Error Calculation : 18mm Magnet

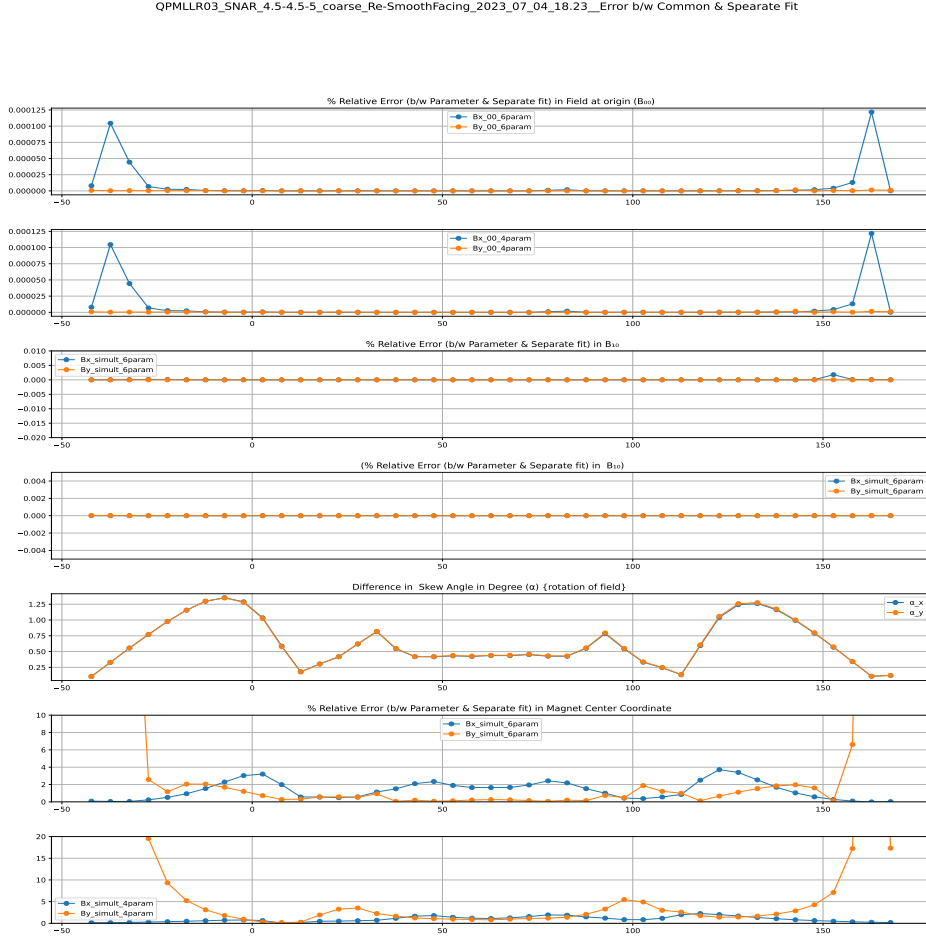


Figure 4.6: Error Calculation : 30mm Magnet

4.4 Fitting Including Z-component

Let consider a model function of an ideal quadrupole with variable gradient along its axis. The magnetic scalar potential of an ideal quadrupole (QP) can be written as

$$\begin{aligned}
 V_M(x, y, z) &= -xyG_0(z) - G_1(z)xyr^2 - G_2(z)xyr^4 + \dots \\
 &= -xy \sum_{k=0}^{\infty} (r^2)^k G_k(z)
 \end{aligned} \tag{4.14}$$

where $r^2 = x^2 + y^2$

In order for this function to satisfy the Laplace equation (as a consequence of $\nabla \cdot B = 0$ and $\nabla \times B = 0$), then coefficient $G_k(z)$ in the above equation 4.14 must satisfy:

$$G_{k+1}(z) = \frac{1}{4(k+1)(k+3)} G''_k(z)$$

which implies

$$G_1(z) = \frac{1}{12} G_0'''(z) \quad (4.15)$$

$$G_2(z) = \frac{1}{384} G_0''''(z) \quad (4.16)$$

$$G_k(z) = \frac{2}{4^k k! (k+2)!} G^{(2k)}(z) \quad (4.17)$$

The magnetic fields are obtained via $\mathbf{B} = -\nabla V_M$, by partial differentiation :

$$\begin{aligned} B_x &= G_0(z)y + G_0''(z)(3x^2y + y^3) + \dots \\ B_y &= G_0(z)x + G_0''(z)(x^3 + 3xy^2) + \dots \\ B_z &= G_0'(z)xy + G_0'''(z)(x^3y + xy^3) + \dots \end{aligned} \quad (4.18)$$

For our purposes it will be sufficient to stop the series after the term G_1xyr^2 in the eqn 4.14. Thus, ignoring higher order terms in eqn 4.18 :

$$B_x = G_0(z) \quad B_y = G_0(z)x \quad B_z = G_0'(z)xy \quad (4.19)$$

4.4.1 6 - Parameter Common Fit (All 3 component)

Theoretically equation 4.19 shows that X, Y component follows the same form even after adding Z-component. That's why we looked for more versatile form of fitting discussed in section 4.2.1, where we have included all components of magnetic field.

Earlier we were calculating the intercept, and then deriving magnetic centre in two step. But including Translational correction (X_c , Y_c) to the measurement coordinates make things computationally faster. Translation of Origin can be done as

$$\begin{bmatrix} X' \\ Y' \end{bmatrix} = \begin{bmatrix} X - X_c \\ Y - Y_c \end{bmatrix} \quad (4.20)$$

We have kept equation more or less same for B_x and B_y as eqn 4.1, 4.2 and added the third (B_z) component. So, the modified form as follows :

$$\begin{aligned} B_x &= (B_{10}^x)(X - X_c) + (B_{01}^x)(Y - Y_c) \\ B_y &= (B_{10}^y)(X - X_c) + (B_{01}^y)(Y - Y_c) \\ B_z &= G_0'(z)(X - X_c)(Y - Y_c) \end{aligned} \quad (4.21)$$

Further parameters like Skew angle, Gradient can be calculated as described in the eqn 4.9. As we have modified the fitting functions, we can directly obtain values of Magnetic Centre from the equations itself.

4.4.2 4 - Parameter Common Fit (All 3 component)

Now, we will consider Rotational transform along with Translation mentioned as above. First we consider the translation of the origin and then we will consider there is a rotation in the measurement coordinate system. Let's say X', Y' be the

ideal coordinate system satisfying the eqn 4.4. Transformation of Ideal coordinates to Measurement coordinates can be shown as :

$$\begin{bmatrix} X' \\ Y' \end{bmatrix} = \begin{bmatrix} \cos(\alpha) & -\sin(\alpha) \\ \sin(\alpha) & \cos(\alpha) \end{bmatrix} \begin{bmatrix} X - X_c \\ Y - Y_c \end{bmatrix} \quad (4.22)$$

As equation for X, Y component remains unchanged, we will follow eqn 4.6 with a slight modification. Fitting equation will be

$$\begin{aligned} B_x &= G_0[\sin(\alpha)(X - X_c) + \cos(\alpha)(Y - Y_c)] \\ B_y &= G_0[\cos(\alpha)(X - X_c) - \sin(\alpha)(Y - Y_c)] \\ B_z &= G'_0[\cos(2\alpha)(X - X_c)(Y - Y_c) + \frac{1}{2}\sin(2\alpha)((X - X_c)^2 - (Y - Y_c)^2)] \end{aligned} \quad (4.23)$$

In both of the method, each component is cascaded one after another as described in eqn 4.11, 4.12 and then fitted with least_square fitting method.

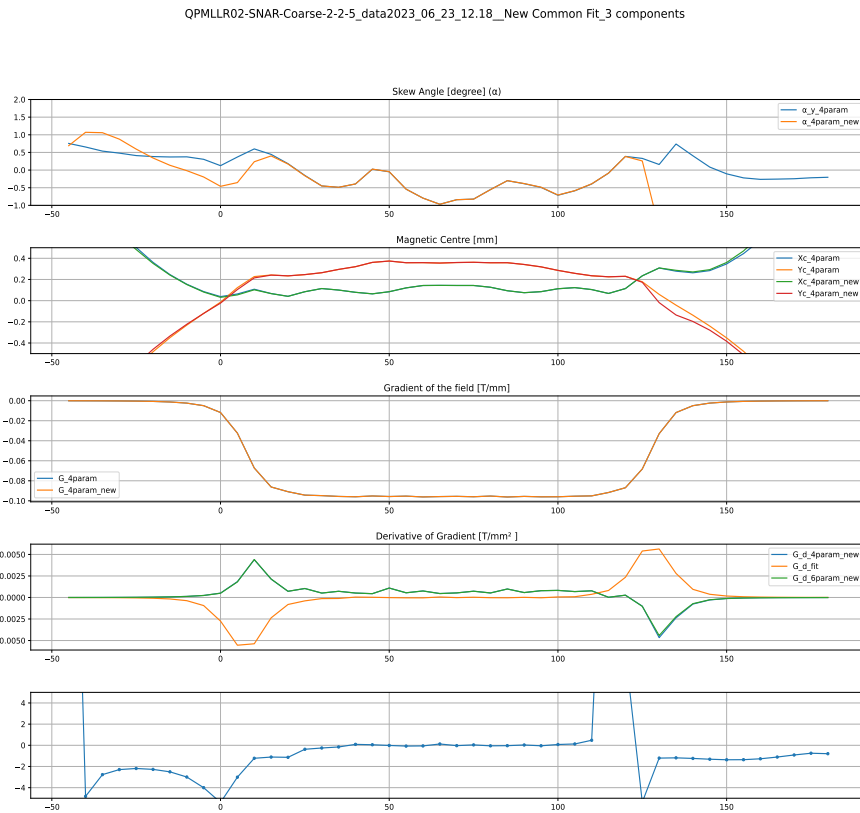


Figure 4.7: Three component fitting : 18mm Magnet

4.4.3 Parameter Calculation

In the above two methods, we have eliminated Field at Origin parameter. In place of that we have included Magnetic Centre coordinate directly in to the fitting function. Rest parameters like Gradient, Skew Angle are calculated as discussed in the section 4.2.3. Here, we have also introduced a new parameter i.e. **Derivative of Gradient**.

First we have calculated the derivative value from the Z-component fitting and then cross-calculated derivative from **Central difference method**[4]. This follows :

$$G'_0(Z) = \frac{\partial G_0}{\partial Z} = \frac{1}{2} \frac{(G_0)_{i+1} - (G_0)_{i-1}}{Z_{i+1} - Z_i} \quad (4.24)$$

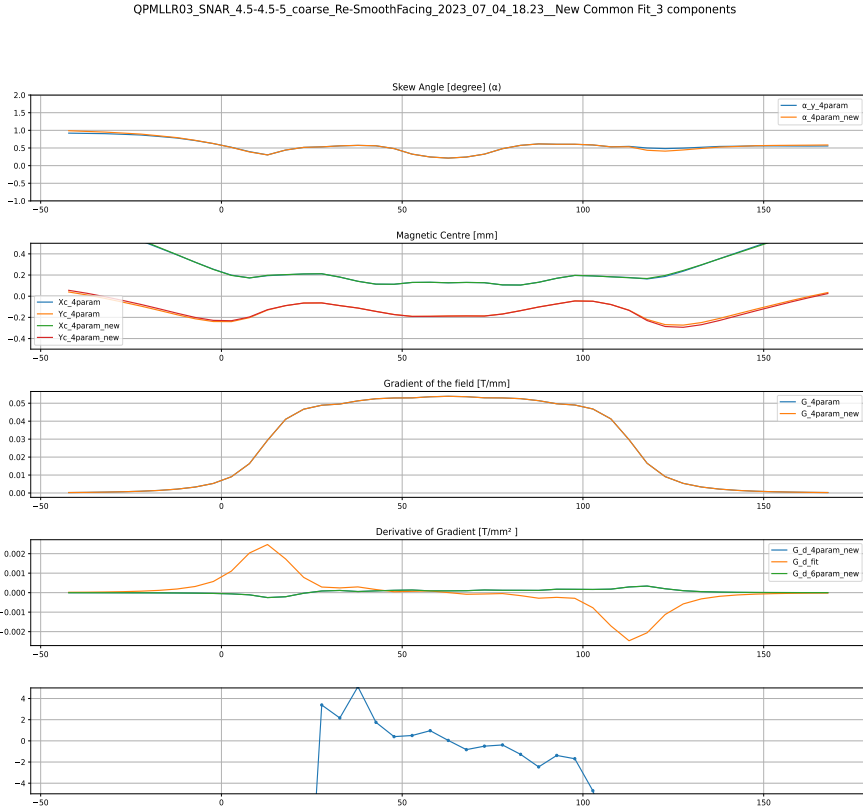


Figure 4.8: Three component fitting : 30mm Magnet

Chapter 5

Advanced Probe Analysis

5.1 Enge Parametrisation

The Enge function can be used to parametrize the field gradient distribution along with the magnet's axis. This function effectively fits the fringe field edge to the ideal field. It is defined as follows :

Let's consider the normal coordinate for magnet axis to be z_n , then Enge Function is defined as

$$f_{enge} = \frac{1}{1 + \exp(C_0 + C_1 z_n + C_2 z_n^2 + C_3 z_n^3)} \quad (5.1)$$

Where C_0, C_1, C_2, C_3 are the unknown coefficients to be determined. Normal coordinates are defined as $z_n = z - z_0$, in which $z_0 = 0$ for the simplicity reason. Basically, z_0 is the overall offset value, which can be initiated to shift the graph on z-axis. We have also assumed $C_0 = 0$ so that, Enge function achieve FWHM (Full width Half Maxima) at $z_n = 0$.

Now, we have the task of defining the Gradient function to satisfy both rise at the entry plane and fall at the exit plane. This can be done by choosing a suitable argument to the Enge Function. Ideally, the Gradient function for a quadrupole magnet looks like **Rectangular function**. In the actual system of bore diameter D, let's define z_l as the entry plane and z_r as the exit plane with maximum gradient value as G_{max} . Thus, the gradient is defined as a function of z as follows

$$\begin{aligned} f_1 &= f_{enge} \left(-\frac{z - z_l}{D} \right) \\ f_2 &= f_{enge} \left(-\frac{z - z_r}{D} \right) \\ G(z) &= G_{max} f_1 f_2 \end{aligned} \quad (5.2)$$

Function $G(z)$ is fitted over the calculated gradient values at each z slices. From the fitting, unknown parameters are calculated as the following table 5.1 and table 5.2.

Date of Measurement	Magnetic Length(mm) ($ z_l - z_r $)	Gradient(T/mm) (G_{max})	C_1	C_2	C_3
2021/11/15	120.7423	-0.0963	4.7246	-0.1766	-0.0835
2021/11/16	120.6025	-0.0959	5.3347	-1.0447	-0.1990
2022/10/12	120.8059	-0.0962	4.0947	-0.1838	-0.0779
2023/06/23	120.6283	-0.0953	5.1577	-0.8817	-0.1680
2023/06/23	120.6556	-0.0952	5.0657	-0.8276	-0.1609

Table 5.1: Enge's Parametrisation for QPM-LLR-02 (18mm)

Date of Measurement	Magnetic Length(mm) ($ z_l - z_r $)	Gradient(T/mm) (G_{max})	C_1	C_2	C_3
2021/09/30	108.4013	-0.0228	8.6396	91.5952	349.6619
2021/09/29	108.1132	-0.0228	8.0772	87.9734	358.75
2022/06/29	102.2989	0.0523	5.1503	-0.8945	-0.3824
2023/07/03	102.4091	-0.0521	5.4918	-1.188	-0.474
2023/07/04	102.3160	0.0523	5.4939	-1.1967	-0.4768

Table 5.2: Enge's Parametrisation for QPM-LLR-03 (30mm)

5.1.1 Power Law fit to Enge's Function

In the Enge function, we have used a **cubic polynomial** in the argument of exponential. In place of a polynomial, we can check for a power law expression (i.e. having less number of constraints). Keeping all other steps of calculation as it is, we will only change argument of enge function as

$$f_{power} = \frac{1}{1 + \exp\{(C.(z_n)^q)\}} \quad (5.3)$$

Where C, q are only two unknown in this case. Unknown values are determined from power law fit is tabulated in the table 5.3 and table 5.4 below.

Date of Measurement	Magnetic Length (mm) ($ z_l - z_r $)	Gradient(T/mm) (G_{max})	C	q
2021/11/15	120.5172	-0.0966	4.0601	0.7865
2021/11/16	120.6877	-0.0965	4.1356	0.7930
2022/10/12	120.8989	-0.0963	4.0195	0.9876
2023/06/23	120.8840	-0.0957	4.2267	0.8498
2023/06/23	120.7767	-0.0957	4.2153	0.8537

Table 5.3: Power Law Parametrisation for QPM-LLR-02 (18mm)

Date of Measurement	Magnetic Length (mm) ($ z_l - z_r $)	Gradient(T/mm) (G_{max})	C	q
2021/09/30	100.2134	-0.0227	57.316	-3.008
2021/09/29	100.0000	-0.0237	3.6901	0.1317
2022/06/29	102.0125	0.0534	3.761	0.7702
2023/07/03	101.6709	-0.0534	3.7442	0.7362
2023/07/04	101.5702	0.0537	3.7416	0.7353

Table 5.4: Power Law Parametrisation for QPM-LLR-03 (30mm)

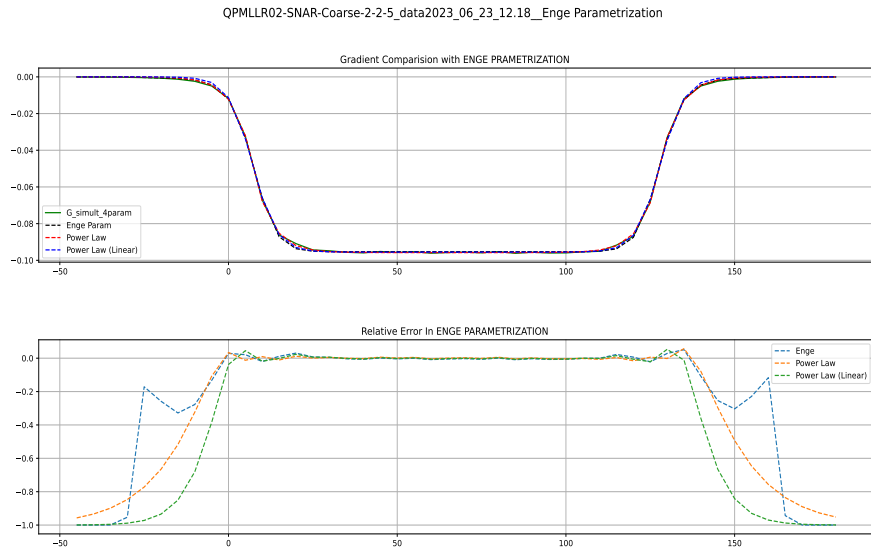


Figure 5.1: Enge Gradient : 18mm Magnet

5.1.2 Linear Power Law Fit

On the verge of reducing constraint in the fitting function, we would like to further eliminate one more degree of freedom in the Power law fit in the eqn 5.3. Keeping Linear polynomial in the argument of exponential function, Fitting function simplified in to

$$f_{linear} = \frac{1}{1 + \exp\{(C.z_n)\}} \quad (5.4)$$

In the next section, we will plot the calculated Gradient values from above three methods and then compare the relative error in the each method with respect to previous Gradient Values.

5.1.3 Results

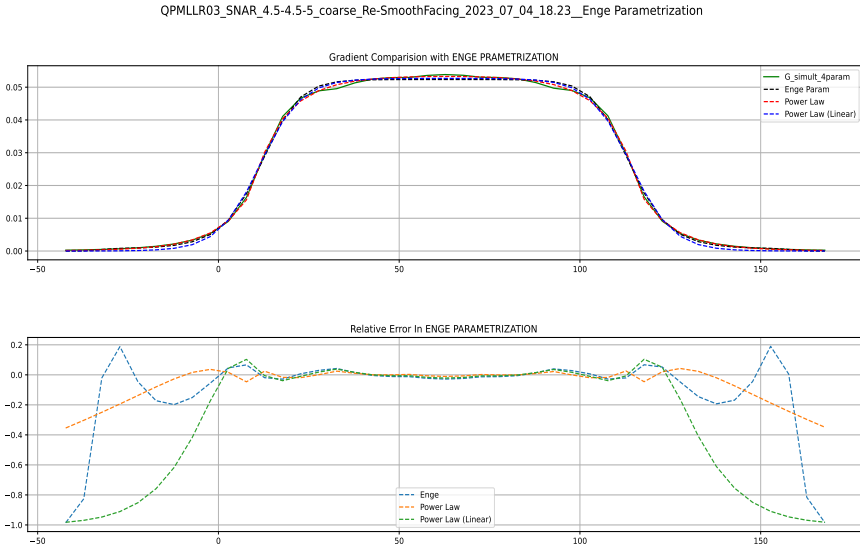


Figure 5.2: Enge Gradient : 30mm Magnet

5.2 Developing Theory for Non-Linear Fit

Till now we have considered the ONLY **Quadrupole** field. Such type of Field is **linearly** dependent on the position coordinate. Though we have calculated non-ideal nature via Skew angle in the probe, our interest still lies in the higher order approximation. It will be of great use, if we can check whether there is any implication from higher orders like Sextupole and Octupole terms.

5.2.1 Method of 2D Taylor Expansion

Following from Quadrupole relation, **Sextupole** will have **squared** dependencies and **Octopole** will have **Cubic** relation over coordinates. Hence, for each order term, we will start taking all possible combination of X, Y coordinates. Considering possible combinations, Sextupole and Octupole will be having number of terms respectively. For any component (whether X or Y) pattern of the equations will remain same, only value of the unknown coefficients will be different. Either of the component has the form as :

$$\begin{aligned}
 \text{Quadrupole term} &= B_{00} + B_{10}X + B_{01}Y \\
 \text{Sextupole term} &= B_{20}X^2 + B_{11}XY + B_{02}Y^2 \\
 \text{Octupole term} &= B_{30}X^3 + B_{21}X^2Y + B_{12}XY^2 + B_{03}Y^3 \\
 \implies B_{x,y} &= \text{Quad term} + \text{Sext term} + \text{Octo term}
 \end{aligned} \tag{5.5}$$

In this method, each component is fitted separately with python command of *curvefit* with respect to corresponding observed value from Hall Probe measurement.

5.2.2 Concept of Multipole Expansion

In another perspective, we will take inference from the field **Multipole Expansion**. A multipole field expansion for the scalar field can be written as :

$$\phi = \sum_{m=0}^{\infty} r^m \{A_m \cos(m\theta) + B_m \sin(m\theta)\} \quad (5.6)$$

where r is the distance from the central axis, θ is the azimuthal angle, and $\theta = 0$ is the standard positive x direction. A_m and B_m are some constant coefficients. This expression is in Polar Coordinate system. We intend to study upto Octupole term. So our subject of interest will be $m = 2, 3, 4$.

For Quadrupole, $m = 2$, that follows

$$\phi = A_2 r^2 \cos(2\theta) + B_2 r^2 \sin(2\theta) \quad (5.7)$$

Rewriting after applying Polar to Cartesian coordinate transformation

$$\phi = A_2(x^2 - y^2) + B_2(xy) \quad (5.8)$$

This gives the Quadrupole field as :

$$\mathbf{B} = -\nabla\phi = A_2(-2x\hat{i} + 2y\hat{j}) + B_2(-2y\hat{i} - 2x\hat{j}) \quad (5.9)$$

NOTE : In this way of field determination, $A_2 = 0$ gives the normal quadrupole, and $B_2 = 0$ gives the skew quadrupole. This same concept is also applicable to Sextupole and Octupole field discussed below.

When $m = 3$;

$$\phi = A_3 r^3 \cos(3\theta) + B_3 r^3 \sin(3\theta) \quad (5.10)$$

$$= A_3 x^3 - 3A_3 xy^2 + 3B_3 x^2 y + B_3 y^3 \quad (5.11)$$

Taking the partial derivative ; Sextupole field described as :

$$\begin{aligned} \frac{\partial \phi}{\partial x} &= B_x = \hat{i}[(-3A_3)x^2 + (-6B_3)xy + (3A_3)y^2] \\ \frac{\partial \phi}{\partial y} &= B_y = \hat{j}[(-3B_3)x^2 + (6A_3)xy + (3B_3)y^2] \end{aligned} \quad (5.12)$$

Similarly when $m = 4$;

$$\phi = A_4 r^4 \cos(4\theta) + B_4 r^4 \sin(4\theta) \quad (5.13)$$

$$= A_4 x^4 + A_4 y^4 - 6A_4 x^2 y^2 + 4B_4 x^3 y - 4B_4 x y^3 \quad (5.14)$$

Thus Octupole Field comes out to be

$$\begin{aligned} \frac{\partial \phi}{\partial x} &= B_x = \hat{i}[(-4A_4)x^3 + (-12B_4)x^2 y + (12A_4)xy^2 + (4B_4)y^3] \\ \frac{\partial \phi}{\partial y} &= B_y = \hat{j}[(-4B_4)x^3 + (12A_4)x^2 y + (12B_4)xy^2 + (-4A_4)y^3] \end{aligned} \quad (5.15)$$

In general, we will assume that each magnetic poles will be Skewed ones. So, we will be equating coefficients ' \mathbf{A} ' to be zero in equations mentioned above.

5.2.3 Method of Multipole Expansion

Assuming Skewed Poles and taking common coefficients out, each field component expressed as follows

$$B_{x,y} = \text{Quadrupole Term} + \text{Sextupole term} + \text{Octupole term}$$

For B_x component

$$\begin{aligned} \text{Quadrupole Term} &= Gy \\ \text{Sextupole Term} &= 2S(xy) \\ \text{Octupole Term} &= O(-3x^2y + y^3) \end{aligned} \tag{5.16}$$

For B_y component

$$\begin{aligned} \text{Quadrupole Term} &= Gx \\ \text{Sextupole Term} &= S(x^2 - y^2) \\ \text{Octupole Term} &= O(3xy^2 - x^3) \end{aligned} \tag{5.17}$$

Where, G, S, O are the Gradient values in respective magnetic pole term.

Now considering the above equation, we will include the transformation of coordinate (translation & rotation) in XYZ-plane.

Chapter 6

Conclusion

Bibliography

- [1] *FINDING OPTIMAL ROTATION AND TRANSLATION BETWEEN CORRESPONDING 3D POINTS.* Nghiaho.com.
- [2] K. S. Arun, T. S. Huang, and S. D Blostein. *Least-Squares Fitting of Two 3-D Point Sets*, volume 9. IEEE Transactions on Pattern Analysis and Machine Intelligence, May 1987.
- [3] Kai Hock. *Sextupole magnet*. Cornell University, June 2010.
- [4] D Levy. *Numerical Differentiation*. University of Maryland.
- [5] Andy Wolski. *Maxwell's Equations for Magnets, Part I: Ideal Multipole Fields*. CAS Specialised Course on Magnets Bruges, Belgium, June, 2009.